



# Differential effects of simvastatin on membrane organization and dynamics in varying phases

Subhashree Shubhrasmita Sahu, Parijat Sarkar, Sandeep Shrivastava, Amitabha Chattopadhyay\*

CSIR-Centre for Cellular and Molecular Biology, Uppal Road, Hyderabad, 500 007, India

## ARTICLE INFO

### Keywords:

DPH  
TMA-DPH  
Simvastatin  
Membrane phase  
Membrane order

## ABSTRACT

Simvastatin belongs to the statin family of cholesterol lowering drugs which act as competitive inhibitors of HMG-CoA reductase, the rate-determining enzyme in cholesterol biosynthesis pathway. Simvastatin is a semi-synthetic, highly lipophilic statin, and has several side effects. Since HMG-CoA reductase is localized in the endoplasmic reticulum, orally administered simvastatin needs to cross the cellular plasma membrane to be able to act on HMG-CoA reductase. With an overall goal of exploring the interaction of simvastatin with membranes, we examined the effect of simvastatin on the organization and dynamics in membranes of varying phase, in a depth-dependent manner. For this, we employed DPH and TMA-DPH, which represent fluorescent membrane probes localized at two different locations (depths) in the membrane. Analysis of fluorescence anisotropy and lifetime data of these depth-specific probes in membranes of varying phase (gel/fluid/liquid-ordered) showed that the maximum membrane disordering was observed in gel phase, while moderate effects were observed in liquid-ordered phase, with no significant change in membrane order in fluid phase membranes. We conclude that simvastatin induces change in membrane order in a depth-dependent and phase-specific manner. These results provide novel insight in the membrane interaction of simvastatin and could be crucial for understanding its pharmacological effect.

## 1. Introduction

Statins are competitive inhibitors of HMG-CoA reductase (Istvan and Deisenhofer, 2001; Endo, 2008; Stossel, 2008), the key enzyme in the rate-limiting step of cholesterol biosynthesis pathway (Goldstein and Brown, 1990). HMG-CoA reductase converts HMG-CoA into mevalonate, which is the biosynthetic precursor of membrane cholesterol and other important isoprenoids necessary for protein prenylation (Goldstein and Brown, 1990; Menge et al., 2005). Statins are one of the top selling drugs globally and are commonly used as cholesterol lowering drugs for hypercholesterolemia and dyslipidemia (Menge et al., 2005).

Simvastatin is a semi-synthetic, highly lipophilic statin (Serajuddin et al., 1991; Sarr et al., 2008), and is believed to be one of the most effective statins (Schaefer et al., 2004). It contains a decaline moiety, a lactone ring (resembling HMG) and a short hydrocarbon chain (see Fig. 1a). Simvastatin is orally administered as an inactive lactone form, which gets hydrolyzed to its active  $\beta$ -hydroxy acid form in the liver

(Slater and MacDonald, 1988; Serajuddin et al., 1991). An advantage for using simvastatin as a cholesterol-lowering drug is its gamut of beneficiary effects in the nervous system (Menge et al., 2005; Kolovou et al., 2008; Wu et al., 2008, 2012; Li et al., 2009). On the other hand, it has adverse side effects such as myotoxicity, sleeping disorder and depression (Saheki et al., 1994; Ozek et al., 2010, 2014; Cham et al., 2016). Several studies have been carried out to elucidate the mechanism underlying the side effects associated with simvastatin administration (Liao and Laufs, 2005; Ramkumar et al., 2016; Mach et al., 2018). Possible reasons for the side effects include the inhibition of isoprenoid synthesis (Liao, 2002; Rikitake and Liao, 2005) that serves as an important post-translational modification for a variety of membrane anchored proteins (Van Aelst and D'souza-Schorey, 1997; Liao and Laufs, 2005). In addition, it has been shown that simvastatin induces lipid peroxidation and decrease in acyl chain unsaturation, leading to changes in lipid composition and concentration (Garip and Severcan, 2010). Since statins are a group of amphipathic drugs, prior to interaction with HMG-CoA reductase and exhibiting its intracellular

**Abbreviations:** DMPC, 1,2-dimyristoyl-*sn*-glycero-3-phosphocholine; DPH, 1,6-diphenyl-1,3,5-hexatriene; DPPC, 1,2-dipalmitoyl-*sn*-glycero-3-phosphocholine; HMG-CoA reductase, 3-hydroxy-3-methylglutaryl-coenzyme A reductase; LUV, large unilamellar vesicle; POPC, 1-palmitoyl-2-oleoyl-*sn*-glycero-3-phosphocholine; TMA-DPH, 1-[4-(trimethylammonio)phenyl]-6-phenyl-1,3,5-hexatriene

\* Corresponding author.

E-mail address: [amit@ccmb.res.in](mailto:amit@ccmb.res.in) (A. Chattopadhyay).

<https://doi.org/10.1016/j.chemphyslip.2019.104831>

Received 10 August 2019; Received in revised form 15 September 2019; Accepted 20 September 2019

Available online 27 September 2019

0009-3084/ © 2019 Elsevier B.V. All rights reserved.

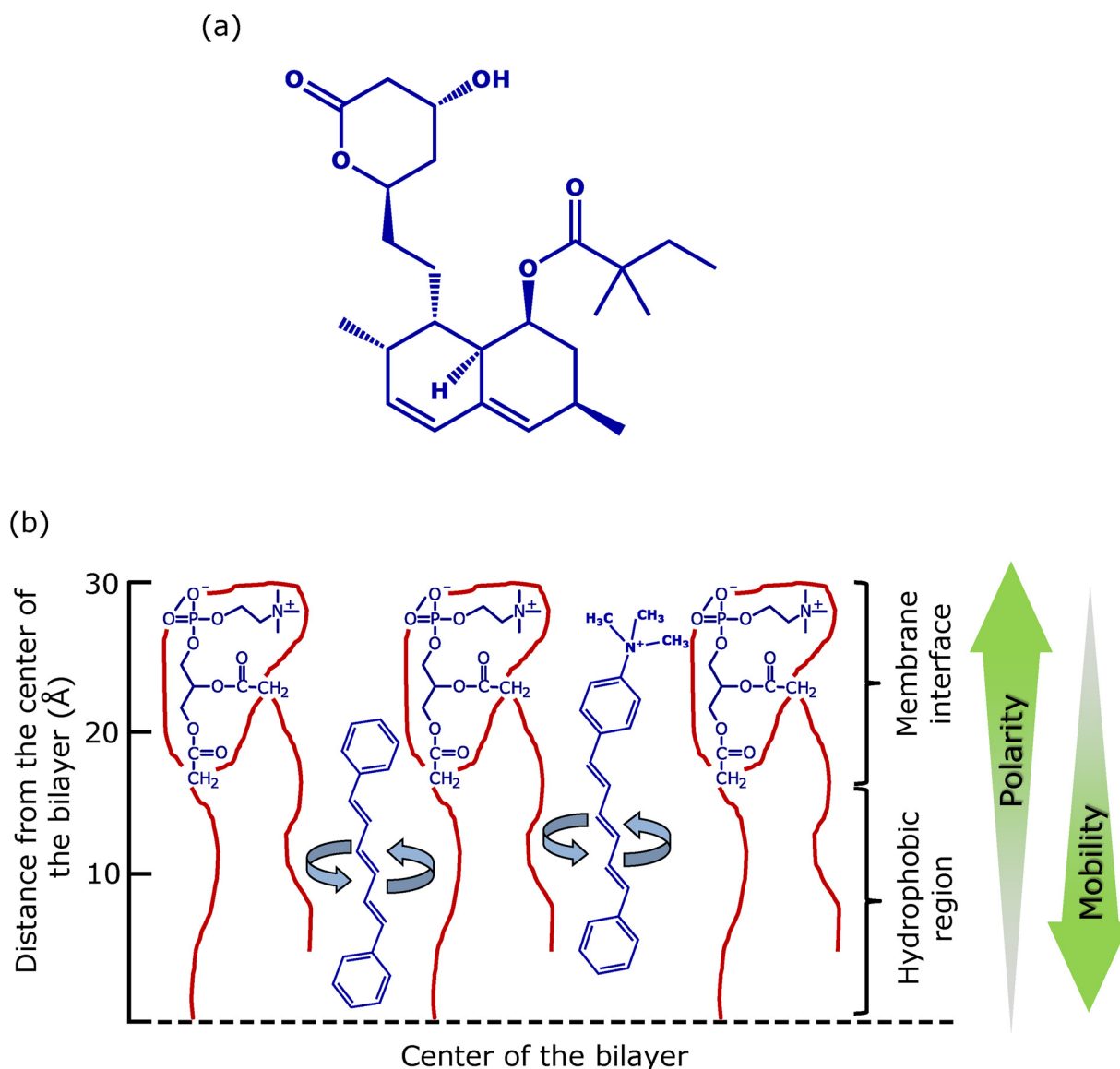


**Fig. 1.** (a) The chemical structure of simvastatin. (b) A schematic representation showing chemical structures and locations of the fluorescent probes DPH and TMA-DPH in a leaflet of the membrane bilayer. The membrane locations of the DPH groups in these compounds are shown according to Kaiser and London (1998). The mobility and polarity gradients along the bilayer normal are also shown (see text for more details). The horizontal line at the bottom indicates the center of the bilayer.

effects, they encounter the membrane bilayer and exert effect on membrane physical properties (Mason et al., 2005; Galiullina et al., 2017; Sariisik et al., 2019).

Study of phase behavior in membranes assumes biological relevance since lateral heterogeneities in membrane order induce distinct nanodomains. Although there is considerable debate on the underlying mechanisms generating such nanodomains (Sevcsik and Schütz, 2015; Goñi, 2019), there is consensus on the role of membrane phase in membrane domain formation and maintenance (van Meer et al., 2008). Since the membrane bilayer represents a *quasi*-two-dimensional anisotropic fluid with distinct polarity and mobility gradients along the bilayer normal (*z*-axis; see Fig. 1b) (Haldar et al., 2011; Pal and Chattopadhyay, 2017), perturbations in membrane order due to interaction with a membrane-active agent may not be confined to a specific location (depth) in the membrane. Membrane order in such cases is often measured in a depth-dependent manner (*i.e.*, in more than one location (depth) along the *z*-axis of the bilayer).

In this paper, we explored the effect of simvastatin on the organization and dynamics in membranes of varying phase utilizing depth-

dependent fluorescent probes, DPH and TMA-DPH (Fig. 1b). DPH is a rod-like hydrophobic molecule that partitions into the membrane and localizes at a depth of  $\sim 8$  Å from the bilayer center (see Fig. 1b; Kaiser and London, 1998). On the other hand, the amphipathic TMA-DPH is a trimethylammonium (a positively charged moiety linked to one of the phenyl rings) derivative of DPH (Prendergast et al., 1981; Fig. 1b). TMA-DPH partitions at the membrane interface ( $\sim 11$  Å from the bilayer center, Kaiser and London, 1998) with its positive charge anchored to the membrane interface. By measuring fluorescence anisotropy and lifetime of DPH and TMA-DPH, we show here that simvastatin modulates membrane order in a depth-dependent and phase-specific manner. We further show that the disordering effect of simvastatin is highest for gel phase membranes as evident from the reduction in apparent rotational correlation time of DPH and TMA-DPH. Our results are relevant in understanding drug-membrane interaction in the context of membrane physical properties, and could provide useful insight in understanding the mode of action of simvastatin and its side effects.

## 2. Materials and methods

### 2.1. Materials

Cholesterol, DMPC, NaCl, Na<sub>2</sub>HPO<sub>4</sub> and NaH<sub>2</sub>PO<sub>4</sub> were obtained from Sigma Chemical Co. (St. Louis, MO). Simvastatin was purchased from Calbiochem (San Diego, CA). DPH and TMA-DPH were purchased from Molecular Probes/Invitrogen (Eugene, OR). POPC and DPPC were purchased from Avanti Polar Lipids (Alabaster, AL). The purity of phospholipids was verified by performing thin layer chromatography on plates pre-coated with silica gel (Merck, Darmstadt, Germany) using chloroform/methanol/water (65:35:5, v/v/v) as the solvent system. All lipids gave a single spot upon developing the TLC plate using a phosphate-sensitive spray followed by charring (Baron and Coburn, 1984). Phosphate assay was carried out to estimate the concentration of phospholipids by complete oxidation with perchloric acid using Na<sub>2</sub>HPO<sub>4</sub> as standard (McClare, 1971). We used DMPC as an internal standard for assessing lipid digestion. DPH and TMA-DPH stocks were prepared in methanol and their concentrations were determined from the molar extinction coefficient ( $\epsilon$ ) of 88,000 M<sup>-1</sup> cm<sup>-1</sup> at 350 nm (Haugland, 1996). Spectroscopic grade solvents were used for all experiments. Water was purified through a Millipore (Bedford, MA) Milli-Q system and used throughout.

### 2.2. Sample preparation

Large unilamellar vesicles (LUVs) of 100 nm diameter were prepared by extrusion technique (MacDonald et al., 1991) using an Avanti Liposfast Extruder (Alabaster, AL), as described previously (Shrivastava et al., 2016). For preparing LUVs, 320 nmol of POPC, DPPC or POPC/40 mol% cholesterol with 3.2 nmol (1 mol%) of DPH or TMA-DPH were co-dried with varying concentration of simvastatin (0–30 mol%). The optical density of the samples measured at 358 nm was less than 0.15 in all cases. Prior to fluorescence measurements, samples were kept in dark for 1 h at room temperature (~23 °C) for equilibration. All experiments were performed with at least three sets of samples at room temperature (~23 °C).

### 2.3. Steady state fluorescence measurements

Steady state fluorescence anisotropy measurements were carried out using a Hitachi F-7000 spectrofluorometer (Tokyo, Japan) with a Hitachi High-tech Science polarization accessory as described previously (Shrivastava et al., 2016). To monitor the fluorescence anisotropy of DPH and TMA-DPH, excitation wavelength of 358 nm and emission wavelength of 430 nm were used. The excitation slit was 1 nm while the emission slit was set at 10 nm to avoid any possible photoisomerization of DPH (Chattopadhyay and London, 1984). We calculated fluorescence anisotropy values from the equation (Lakowicz, 2006):

$$r = \frac{I_{VV} - GI_{VH}}{I_{VV} + 2GI_{VH}} \quad (1)$$

where  $I_{VV}$  and  $I_{VH}$  are the background subtracted fluorescence intensities measured with vertically oriented excitation polarizer while the emission polarizer was oriented vertically and horizontally, respectively.  $G$  represents the grating factor and is the ratio of the efficiencies of the detection system for vertically and horizontally polarized light, and is equal to  $I_{HV}/I_{HH}$ .

### 2.4. Time-resolved fluorescence measurements

Fluorescence lifetimes were calculated from time-resolved fluorescence intensity decays using a Delta-D TCSPC system (Horiba Jobin Yvon IBH, Glasgow, UK) with EzTime software version 3.2.2.4 (Horiba Scientific, Edison, NJ) in the time-correlated single photon counting

mode, as described previously (Pal et al., 2018). For excitation source, a pulsed light-emitting diode (DD-370) was used, which runs at a repetition rate of 20 MHz and generates an optical pulse at 370 nm with pulse duration of 1.2 ns. We collected 10,000 photon counts in the peak channel. Emission slit with bandpass of 4 nm was kept for all measurements. In order to compensate for the shape and timing drift during measurements, we alternated the sample and the scatterer after every 10% acquisition. This additionally ensures that the sample is not exposed to the excitation beam for a prolonged period that could lead to photodamage of the probe. Data were collected and analyzed as discussed previously (Pal et al., 2018). Fluorescent intensity decay curves were obtained by deconvoluting with instrument response function obtained using Ludox (colloidal silica). The obtained decay curves were fitted suitably to a biexponential decay function with  $\chi^2$  value less than 1.5. Intensity-averaged mean fluorescence lifetimes were calculated using the equation (Lakowicz, 2006):

$$\langle \tau \rangle = \frac{\alpha_1 \tau_1^2 + \alpha_2 \tau_2^2}{\alpha_1 \tau_1 + \alpha_2 \tau_2} \quad (2)$$

where  $\alpha$  is the pre-exponential factor that corresponds to the fractional contribution of time-resolved decay of a given component with a lifetime of  $\tau$ .

### 2.5. Statistical analysis

Significance levels were calculated using two-tailed unpaired  $t$ -test with 95% confidence interval using GraphPad Prism software, version 4.0 (San Diego, CA). All plots were generated using Microcal Origin version 6.0 (OriginLab, Northampton, MA).

## 3. Results and discussion

### 3.1. Effect of simvastatin on membrane order in membranes of varying phase

Membrane order is a useful indicator for membrane organization and dynamics. In this work, we explored the change in membrane order in membranes of varying phase with increasing simvastatin concentration. Membrane phases are characterized by their lipid packing, which is dependent on the conformation of lipid hydrocarbon chains. In gel phase, the lipids hydrocarbon chains are ordered and extended, since the chains are in all *trans* conformation. On the other hand, lipid acyl chains are fluid and disordered in the liquid-disordered (or fluid) phase since lipid acyl chains are in *gauche* conformation. Between these two phases lies the liquid-ordered phase, which is implicated in membrane domains (Mouritsen, 2010). In this phase, the lipid acyl chains are extended (ordered), similar to the gel phase, yet exhibit high lateral mobility, reminiscent of the fluid phase membrane (van Meer et al., 2008). An essential hallmark of the liquid-ordered phase is the presence of significant amount of cholesterol in the membrane, above a threshold concentration, depending on the nature of the phospholipid(s) (Thewalt and Bloom, 1992; Brown and London, 1998). In this work, we utilized LUVs composed of POPC, DPPC and POPC with 40 mol% cholesterol, as representatives of fluid (disordered), gel (ordered) and liquid-ordered phase membranes, respectively. In order to monitor membrane order in varying phases, we carried out depth-dependent fluorescence anisotropy measurements using DPH and TMA-DPH, which partition at different depths (locations) into the membrane bilayer (see Fig. 1b; Kaiser and London, 1998).

Fig. 2 shows the steady state anisotropy of DPH and TMA-DPH in various membrane phases with increasing concentration of simvastatin. The steady state fluorescence anisotropy of membrane embedded fluorophores (DPH and TMA-DPH) is an indicator of the rotational mobility of these probes that depends on the packing of lipid acyl chains. Fig. 2 shows changes in steady state anisotropy of DPH in (a)

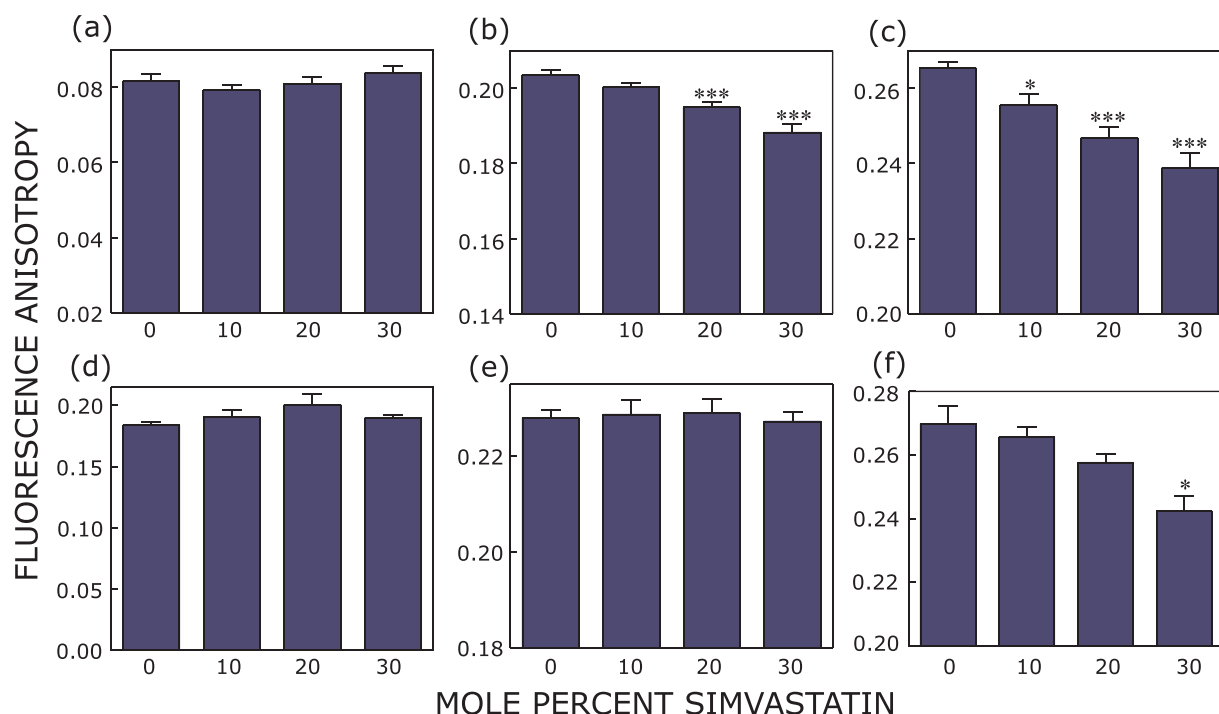


**Fig. 2.** Change in steady state fluorescence anisotropy of DPH in membranes of varying phase: (a) fluid (POPC), (b) liquid-ordered (POPC/40 mol% cholesterol), and (c) gel (DPPC) as a function of increasing concentration of simvastatin. Bottom panels represent fluorescence anisotropy of TMA-DPH in (d) POPC, (e) POPC/40 mol% cholesterol and (f) DPPC membranes with increasing concentration of simvastatin. The excitation and emission wavelengths used were 358 and 430 nm for all measurements. Measurements were performed at room temperature ( $\sim 23^\circ\text{C}$ ). Data represent means  $\pm$  S.E. of at least three independent measurements [\*, \*\*\* represent significant ( $p < 0.05$  and  $p < 0.001$ , respectively) difference in fluorescence anisotropy with respect to control (membranes without simvastatin)]. See Section 2 for other details.

POPC (fluid phase), (b) POPC/40 mol% cholesterol (liquid-ordered phase) and (c) DPPC (gel phase), with increasing simvastatin concentration (0–30 mol%). The steady state anisotropy value for DPH was highest in DPPC (gel phase) membranes ( $\sim 0.265$ ) relative to other phase membranes, since the packing of lipid chains is most tight in this phase. The anisotropy of DPH was  $\sim 0.082$  in POPC (fluid phase) membranes, and  $\sim 0.203$  in liquid-ordered phase membranes. The similarity in DPH anisotropy values between the gel and liquid-ordered phases is to be noted, thereby indicating tighter lipid packing in these phases. The anisotropy of DPH exhibited a reduction of  $\sim 7.4\%$  and  $\sim 9.8\%$  in liquid-ordered and gel phases, respectively, in presence of the highest concentration (30 mol%) of simvastatin used. In contrast to this, DPH anisotropy appeared invariant in fluid phase membranes in presence of simvastatin over the same concentration range (0–30 mol%).

As mentioned above, in order to comprehensively monitor membrane order in membranes of varying phase with increasing simvastatin concentration, we examined the change in membrane order at a shallow location in the membrane using TMA-DPH, in which the DPH moiety is localized at the membrane interface (Kaiser and London, 1998). Fig. 2(d–f) shows that fluorescence anisotropy of TMA-DPH is in general higher in all membrane phases relative to DPH anisotropy values in corresponding membrane phases. This is due to the shallow membrane location of the DPH moiety in TMA-DPH, as reported earlier (Kaiser and London, 1998) and is consistent with the mobility gradient along the bilayer normal in fluid phase membranes (Haldar et al., 2011; Pal and Chattopadhyay, 2017). The reduction in steady state anisotropy of TMA-DPH in presence of maximum concentration of simvastatin was highest ( $\sim 10.4\%$ ) in gel phase membranes (Fig. 2f). The anisotropy of TMA-DPH did not display significant variation in presence of simvastatin (0–30 mol%) in liquid-ordered and fluid phase membranes.

### 3.2. Effect of simvastatin on fluorescence lifetime of DPH and TMA-DPH in varying membrane phases

Fluorescence lifetime is a sensitive indicator of fluorophore micro-environment (Prendergast, 1991). Fluorescence lifetimes of DPH and TMA-DPH are known to be sensitive to polarity in their surrounding membrane environment (Stubbs et al., 1995; Shrivastava et al., 2008) and their lifetime gets reduced with increasing environmental polarity. The fluorescence lifetimes of DPH and TMA-DPH in varying phases of membranes with increasing simvastatin concentration are shown in Tables 1 and 2, respectively. We calculated the intensity-averaged mean fluorescence lifetimes of DPH and TMA-DPH under these conditions from data shown in Tables 1 and 2 using Eq. (2), and the values are represented in Fig. 3. Mean fluorescence lifetimes of both probes exhibited a reduction from gel to fluid phase membranes, thereby indicating more polar environment in the fluid phase, possibly due to increased water penetration in the fluid phase due to loose acyl chain packing. In general, the mean fluorescence lifetime of DPH was found to be higher relative to TMA-DPH in all phases of membranes, which indicates more polar environment at the shallow region where the DPH group in TMA-DPH was localized (Kaiser and London, 1998), possibly due to more water penetration (Stubbs et al., 1995).

The intensity-averaged mean fluorescence lifetime of DPH was highest ( $> 10$  ns) in liquid-ordered and gel phase membranes (Fig. 3b, c), due to tighter acyl chain packing in these membranes. In liquid-disordered (POPC) phase (Fig. 3a), the mean fluorescence lifetime of DPH was shorter ( $\sim 8.5$  ns). Fig. 3(a–c) shows that the mean fluorescence lifetime did not change significantly with increasing concentration of simvastatin, irrespective of the membrane phase. The corresponding change in mean fluorescence lifetime of TMA-DPH with increasing simvastatin concentration is shown in Fig. 3(d–f). The mean fluorescence lifetime of TMA-DPH in fluid and liquid-ordered phase membranes shows no significant change with varying simvastatin

**Table 1**  
Representative fluorescence lifetimes of DPH with increasing simvastatin concentration<sup>a</sup>

mol% simvastatin	$\alpha_1$	$\tau_1$ (ns)	$\alpha_2$	$\tau_2$ (ns)
<b>POPC (Fluid)</b>				
0	0.14	3.95	0.86	8.80
10	0.14	4.12	0.86	8.84
20	0.13	4.02	0.87	8.92
30	0.15	4.00	0.85	8.97
<b>POPC/40 mol% cholesterol (Liquid-ordered)</b>				
0	0.03	4.72	0.97	10.53
10	0.01	4.78	0.99	10.61
20	0.01	4.72	0.99	10.54
30	0.02	4.72	0.98	10.50
<b>DPPC (Gel)</b>				
0	0.04	4.68	0.96	10.81
10	0.05	4.78	0.95	11.01
20	0.07	4.61	0.93	10.90
30	0.05	2.37	0.95	10.75

<sup>a</sup> The excitation wavelength was 370 nm and emission was monitored at 430 nm. The number of photons collected at the peak channel was 10,000. All other conditions are as in Fig. 2. See Section 2 for other details.

**Table 2**  
Representative fluorescence lifetimes of TMA-DPH with increasing simvastatin concentration<sup>a</sup>

mol% simvastatin	$\alpha_1$	$\tau_1$ (ns)	$\alpha_2$	$\tau_2$ (ns)
<b>POPC (Fluid)</b>				
0	0.32	1.41	0.68	4.96
10	0.33	1.53	0.67	4.93
20	0.32	1.55	0.68	4.90
30	0.32	1.55	0.68	4.87
<b>POPC/40 mol% cholesterol (Liquid-ordered)</b>				
0	0.13	3.81	0.87	8.35
10	0.11	3.87	0.89	8.47
20	0.12	3.86	0.88	8.43
30	0.13	3.98	0.87	8.40
<b>DPPC (Gel)</b>				
0	0.19	1.77	0.81	7.57
10	0.29	3.32	0.71	7.75
20	0.31	3.24	0.69	7.45
30	0.32	3.01	0.68	6.94

<sup>a</sup> The excitation wavelength was 370 nm and emission was monitored at 430 nm in all cases. The number of photons collected at the peak channel was 10,000. All other conditions are as in Fig. 2. See Section 2 for other details.

concentration (see Fig. 3d, e). However, the mean fluorescence lifetime of TMA-DPH is higher (~8 ns) in liquid-ordered phase relative to the corresponding lifetime in fluid phase membranes (~4.5 ns). This implies tighter packing of lipid acyl chains in the liquid-ordered phase, which would reduce water penetration in the membrane. Interestingly, the lifetime of TMA-DPH in gel phase membranes displayed a progressive reduction with increasing simvastatin concentration (Fig. 3f), with a reduction of ~11.7% in mean fluorescence lifetime at the highest concentration of simvastatin used. This could indicate that the tight packing in the gel phase membrane at the interfacial region (where the DPH moiety of TMA-DPH is localized) is disordered in presence of simvastatin, thereby increasing water penetration and membrane polarity around TMA-DPH. The absence of this effect in gel phase membranes when DPH was used as a probe (Fig. 3c) could be indicative of differential localization of the DPH group in these cases (Fig. 1b), keeping in mind the interfacial localization of simvastatin in the membrane (Mason et al., 2005).

### 3.3. Effect of simvastatin on apparent rotational correlation times of DPH and TMA-DPH in membranes of varying phase

In order to ensure that fluorescence anisotropy values reported in Fig. 2 were not affected by lifetime artifacts, we calculated apparent rotational correlation times using Perrin's equation (Lakowicz, 2006):

$$\tau_e = \frac{\langle \tau \rangle r}{r_0 - r} \quad (3)$$

where  $r_0$  is the fundamental anisotropy (the fluorescence anisotropy of a fluorophore in the absence of any depolarizing processes),  $r$  represents the steady state fluorescence anisotropy (from Fig. 2) and  $\langle \tau \rangle$  is the mean fluorescence lifetime (Fig. 3). Fig. 4 shows the apparent rotational correlation times estimated from Eq. (3) using a value of  $r_0$  of 0.36 for DPH (Shinitzky and Barenholz, 1974). The apparent rotational correlation times of DPH and TMA-DPH in gel phase membrane were highest (~29 and 22 ns, respectively) indicating maximum motional restriction experienced by probes in gel phase membranes (Fig. 4c, f). The loose packing (disorder) in fluid phase membranes gave rise to the lowest values (~2.4 and 4.8 ns in DPH and TMA-DPH, respectively) of apparent rotational correlation time (Fig. 4a, d). The values of apparent rotational correlation time observed for liquid-ordered phase membranes were between these fluid and gel phase membranes (Fig. 4b, e). A comparison of Figs. 2 and 4 shows that the change in apparent rotational correlation times for both DPH and TMA-DPH exhibited more or less similar trend as exhibited for fluorescence anisotropy with increasing simvastatin concentration. This indicates that fluorescence anisotropy measurements are independent of lifetime-induced artifacts. Taken together, these results suggest that simvastatin induces change in membrane order in a depth-dependent and phase-specific manner.

HMG-CoA reductase is a membrane protein in the endoplasmic reticulum with eight membrane spanning segments, with the active catalytic site located in a long cytoplasmic carboxyl terminal domain (Istvan and Deisenhofer, 2001; Jo and DeBose-Boyd, 2010). A crucial requirement for statins, prior to exhibiting their intracellular effects, is that they should be capable of crossing the plasma membrane. The overall goal of the present study was to explore the effect of simvastatin on the organization and dynamics of membranes representing various membrane phases. Membrane order is a key determinant of membrane protein function (Fong and McNamee, 1986, 1987; Rao et al., 2016). Previous studies reported that simvastatin has a high octanol-water partition coefficient relative to other hydrophilic statins (Serajuddin et al., 1991) that allows it to partition into model membranes (Mason et al., 2005; Galiullina et al., 2017; Sariisik et al., 2019) and cross the blood-brain-barrier (Saheki et al., 1994; Wood et al., 2010; Sierra et al., 2011). However, information on localized changes in membrane order along the bilayer normal in various membrane phases was lacking. In this work, we monitored the location-specific dynamic changes by utilizing two fluorescent membrane probes DPH and TMA-DPH. Analysis of rotational dynamics of these fluorescent probes provides depth-dependent information on membrane interaction of simvastatin that gets partitioned into the membrane. We measured such depth-specific membrane order across various membrane phases that play a crucial role in membrane organization and domain formation (van Meer et al., 2008; Saxena et al., 2015). Our results show that maximum disordering was induced in gel phase membranes, followed by moderate effects in liquid-ordered membranes, while no significant change in membrane order was observed for fluid phase membranes. Our results provide novel insight in the interaction of simvastatin with membranes, which could be crucial for its pharmacological activity and deciphering its pleiotropic effects.

### Declaration of Competing Interest

The authors declare that there is no conflict of interest.

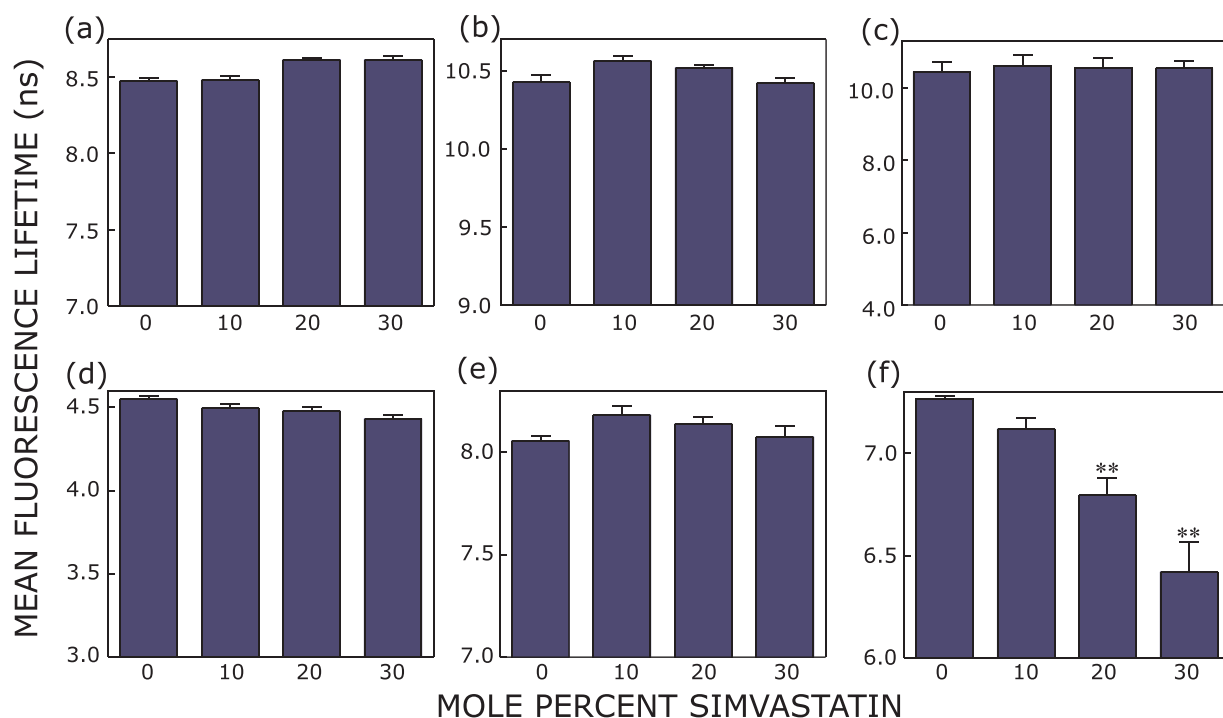


**Fig. 3.** The mean intensity-averaged fluorescence lifetime of DPH in membranes of varying phases: (a) fluid (POPC), (b) liquid-ordered (POPC/40 mol% cholesterol), and (c) gel (DPPC) as a function of increasing concentration of simvastatin. Bottom panels show the change in fluorescence lifetime of TMA-DPH in (d) POPC, (e) POPC/40 mol% cholesterol and (f) DPPC membrane with increasing concentration of simvastatin. Mean fluorescence lifetimes were calculated from Eq. (2). The excitation and emission wavelengths used were 370 and 430 nm in all cases. Measurements were performed at room temperature ( $\sim 23^\circ\text{C}$ ). Data represent means  $\pm$  S.E. of at least three independent measurements [**\*\*** represent significant ( $p < 0.01$ ) difference in mean fluorescence lifetime with respect to control (membranes without simvastatin)]. See Section 2, and Tables 1 and 2 for more details.

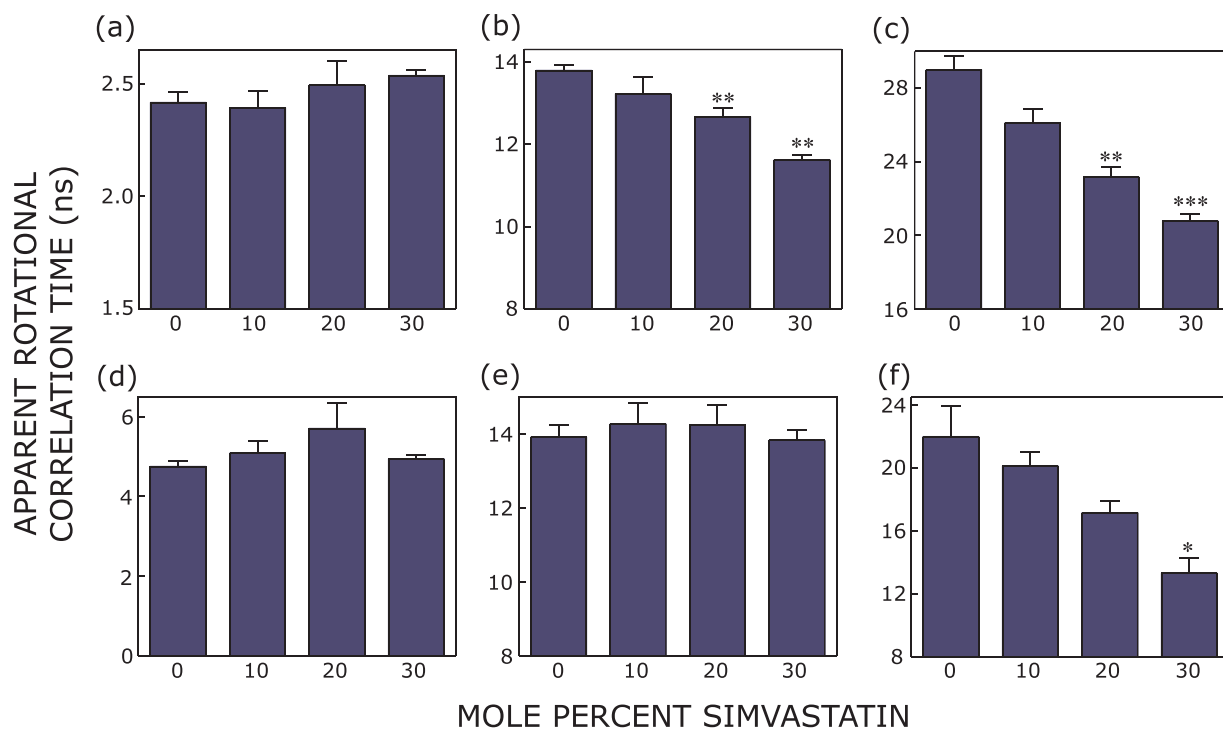


**Fig. 4.** The apparent rotational correlation time of DPH and TMA-DPH in different membrane phases with increasing concentration of simvastatin. Panels (a–c) show changes in apparent rotational correlation time of DPH in fluid (POPC), liquid-ordered (POPC/40 mol% cholesterol), and gel (DPPC) phase membranes, respectively. The apparent rotational correlation time for TMA-DPH in fluid (POPC), liquid-ordered (POPC/40 mol% cholesterol), and gel (DPPC) phase membranes are shown in panels (d–f), respectively. Apparent rotational correlation times were calculated using fluorescence anisotropy values from Fig. 2 and mean fluorescence lifetimes from Fig. 3 using Eq. (3). Values represent means  $\pm$  S.E. of at least three independent calculations [**\***, **\*\***, **\*\*\*** represent significant ( $p < 0.05$ ,  $p < 0.01$  and  $p < 0.001$ , respectively) difference in apparent rotational correlation time with respect to control (membranes without simvastatin)]. See text for other details.

## Acknowledgments

A.C. gratefully acknowledges support from SERB Distinguished Fellowship (Department of Science and Technology, Govt. of India). P.S. thanks the Council of Scientific and Industrial Research for the award of a Shyama Prasad Mukherjee Fellowship. A.C. is a Distinguished Visiting Professor at the Indian Institute of Technology Bombay (Mumbai), and Adjunct Professor at the Tata Institute of Fundamental Research (Mumbai), RMIT University (Melbourne, Australia), and Indian Institute of Science Education and Research (Kolkata), and an Honorary Professor at the Jawaharlal Nehru Centre for Advanced Scientific Research (Bengaluru). We thank members of the Chattopadhyay laboratory for critically reading the manuscript.

## References

- Baron, C.B., Coburn, R.F., 1984. Comparison of two copper reagents for detection of saturated and unsaturated neutral lipids by charring densitometry. *J. Liq. Chromatogr.* 7, 2793–2801.
- Brown, D.A., London, E., 1998. Structure and origin of ordered lipid domains in biological membranes. *J. Membr. Biol.* 164, 103–114.
- Cham, S., Koslik, H.J., Golomb, B.A., 2016. Mood, personality, and behavior changes during treatment with statins: a case series. *Drug. Saf. Case Rep.* 3, 1.
- Chattopadhyay, A., London, E., 1984. Fluorimetric determination of critical micelle concentration avoiding interference from detergent charge. *Anal. Biochem.* 139, 408–412.
- Endo, A., 2008. A gift from nature: the birth of the statins. *Nat. Med.* 14, 1050–1052.
- Fong, T.M., McNamee, M.G., 1986. Correlation between acetylcholine receptor function and structural properties of membranes. *Biochemistry* 25, 830–840.
- Fong, T.M., McNamee, M.G., 1987. Stabilization of acetylcholine receptor secondary structure by cholesterol and negatively charged phospholipids in membranes. *Biochemistry* 26, 3871–3880.
- Galiullina, L.F., Aganova, O.V., Latfullin, I.A., Musabirova, G.S., Aganov, A.V., Klochkov, V.V., 2017. Interaction of different statins with model membranes by NMR data. *Biochim. Biophys. Acta* 1859, 295–300.
- Garip, S., Severcan, F., 2010. Determination of simvastatin-induced changes in bone composition and structure by Fourier transform infrared spectroscopy in rat animal model. *J. Pharm. Biomed. Anal.* 52, 580–588.
- Goldstein, J.L., Brown, M.S., 1990. Regulation of the mevalonate pathway. *Nature* 343, 425–430.
- Goñi, F.M., 2019. Rafts: a nickname for putative transient nanodomains. *Chem. Phys. Lipids* 218, 34–39.
- Haldar, S., Chaudhuri, A., Chattopadhyay, A., 2011. Organization and dynamics of membrane probes and proteins utilizing the red edge excitation shift. *J. Phys. Chem. B* 115, 5693–5706.
- Haugland, R.P., 1996. *Handbook of Fluorescent Probes and Research Chemicals*, 6th ed. Molecular Probes, Eugene, OR.
- Istvan, E.S., Deisenhofer, J., 2001. Structural mechanism for statin inhibition of HMG-CoA reductase. *Science* 292, 1160–1164.
- Jo, Y., Debose-Boyd, R.A., 2010. Control of cholesterol synthesis through regulated ER-associated degradation of HMG CoA reductase. *Crit. Rev. Biochem. Mol. Biol.* 45, 185–198.
- Kaiser, R.D., London, E., 1998. Location of diphenylhexatriene (DPH) and its derivatives within membranes: comparison of different fluorescence quenching analyses of membrane depth. *Biochemistry* 37, 8180–8190.
- Kolovou, G.D., Vasiliadis, I., Anagnostopoulou, K., Cokkino, D.V., 2008. Simvastatin: two decades in a circle. *Cardiovasc. Ther.* 26, 166–178.
- Lakowicz, J.R., 2006. *Principles of Fluorescence Spectroscopy*, 3rd ed. Springer, New York.
- Li, B., Mahmood, A., Lu, D., Wu, H., Xiong, Y., Qu, C., Chopp, M., 2009. Simvastatin attenuates microglial cells and astrocyte activation and decreases interleukin-1 $\beta$  level after traumatic brain injury. *Neurosurgery* 65, 179–186.
- Liao, J.K., 2002. Isoprenoids as mediators of the biological effects of statins. *J. Clin. Invest.* 110, 285–288.
- Liao, J.K., Laufs, U., 2005. Pleiotropic effects of statins. *Annu. Rev. Pharmacol. Toxicol.* 45, 89–118.
- MacDonald, R.C., MacDonald, R.I., Menco, B.P.M., Takeshita, K., Subbarao, N.K., Hu, L.-R., 1991. Small-volume extrusion apparatus for preparation of large, unilamellar vesicles. *Biochim. Biophys. Acta* 1061, 297–303.
- Mach, et al., 2018. Adverse effects of statin therapy: perception vs. the evidence - focus on glucose homeostasis, cognitive, renal and hepatic function, haemorrhagic stroke and cataract. *Eur. Heart J.* 39, 2526–2539.
- Mason, R.P., Walter, M.F., Day, C.A., Jacob, R.F., 2005. Intermolecular differences of 3-hydroxy-3-methylglutaryl coenzyme A reductase inhibitors contribute to distinct pharmacologic and pleiotropic actions. *Am. J. Cardiol.* 96, 11F–23F.
- McClare, C.W.F., 1971. An accurate and convenient organic phosphorus assay. *Anal. Biochem.* 39, 527–530.
- Menge, T., Hartung, H.-P., Stüve, O., 2005. Statins - a cure-all for the brain? *Nat. Rev. Neurosci.* 6, 325–331.
- Mouritsen, O.G., 2010. The liquid-ordered state comes of age. *Biochim. Biophys. Acta* 1798, 1286–1288.
- Ozek, N.S., Sara, Y., Onur, R., Severcan, F., 2010. Low dose simvastatin induces compositional, structural and dynamic changes in rat skeletal extensor digitorum longus muscle tissue. *Biosci. Rep.* 30, 41–50.
- Ozek, N.S., Bal, I.B., Sara, Y., Onur, R., Severcan, F., 2014. Structural and functional characterization of simvastatin-induced myotoxicity in different skeletal muscles. *Biochim. Biophys. Acta* 1840, 406–415.
- Pal, S., Chattopadhyay, A., 2017. What is so unique about biomembrane organization and dynamics? In: *Chattoadhyay, A. (Ed.), Membrane Organization and Dynamics*. Springer Series in Biophysics. Springer International Publishing, pp. 1–9.
- Pal, S., Aute, R., Sarkar, P., Bose, S., Deshmukh, M.V., Chattopadhyay, A., 2018. Constrained dynamics of the sole tryptophan in the third intracellular loop of the serotonin<sub>1A</sub> receptor. *Biophys. Chem.* 240, 34–41.
- Prendergast, F.G., 1991. Time-resolved fluorescence techniques: methods and applications in biology. *Curr. Opin. Struct. Biol.* 1, 1054–1059.
- Prendergast, F.G., Haugland, R.P., Callahan, P.J., 1981. 1-[4-(Trimethylamino)phenyl]-6-phenylhexa-1,3,5-triene: synthesis, fluorescence properties, and use as a fluorescence probe of lipid bilayers. *Biochemistry* 20, 7333–7338.
- Ramkumar, S., Raghunath, A., Raghunath, S., 2016. Statin therapy: review of safety and potential side effects. *Acta Cardiol. Sin.* 32, 631–639.
- Rao, B.D., Shrivastava, S., Chattopadhyay, A., 2016. Effect of local anesthetics on serotonin<sub>1A</sub> receptor function. *Chem. Phys. Lipids* 201, 41–49.
- Rikitake, Y., Liao, J.K., 2005. Rho GTPases, statins, and nitric oxide. *Circ. Res.* 97, 1232–1235.
- Saheki, A., Terasaki, T., Tamai, I., Tsuji, A., 1994. *In vivo* and *in vitro* blood-brain barrier transport of 3-hydroxy-3-methylglutaryl coenzyme A (HMG-CoA) reductase inhibitors. *Pharm. Res.* 11, 305–311.
- Sarişik, E., Koçak, M., Baloglu, F.K., Severcan, F., 2019. Interaction of the cholesterol reducing agent simvastatin with zwitterionic DPPC and charged DPPG phospholipid membranes. *Biochim. Biophys. Acta* 1861, 810–818.
- Sarr, F.S., André, C., Guillaume, Y.C., 2008. Statins (HMG-coenzyme A reductase inhibitors)-biomimetic membrane binding mechanism investigated by molecular chromatography. *J. Chromatogr. B* 868, 20–27.
- Saxena, R., Shrivastava, S., Chattopadhyay, A., 2015. Cholesterol-induced changes in hippocampal membranes utilizing a phase-sensitive fluorescence probe. *Biochim. Biophys. Acta* 1848, 1699–1705.
- Schaefer, E.J., McNamara, J.R., Tayler, T., Daly, J.A., Gleason, J.L., Seman, L.J., Ferrari, A., Rubenstein, J.J., 2004. Comparisons of effects of statins (atorvastatin, fluvastatin, lovastatin, pravastatin, and simvastatin) on fasting and postprandial lipoproteins in patients with coronary heart disease versus control subjects. *Am. J. Cardiol.* 93, 31–39.
- Serajuddin, A.T.M., Ranadive, S.A., Mahoney, E.M., 1991. Relative lipophilicities, solubilities, and structure-pharmacological considerations of 3-hydroxy-3-methylglutaryl-coenzyme A (HMG-CoA) reductase inhibitors pravastatin, lovastatin, mevastatin, and simvastatin. *J. Pharm. Sci.* 80, 830–834.
- Sevcsik, E., Schütz, G.J., 2015. With or without rafts? Alternative views on cell membranes. *Bioessays* 38, 129–139.
- Shinitzky, M., Barenholz, Y., 1974. Dynamics of the hydrocarbon layer in liposomes of lecithin and sphingomyelin containing dicytlylphosphate. *J. Biol. Chem.* 249, 2652–2657.
- Shrivastava, S., Paila, Y.D., Dutta, A., Chattopadhyay, A., 2008. Differential effects of cholesterol and its immediate biosynthetic precursors on membrane organization. *Biochemistry* 47, 5668–5677.
- Shrivastava, S., Dutta, D., Chattopadhyay, A., 2016. Effect of local anesthetics on the organization and dynamics in membranes of varying phase: a fluorescence approach. *Chem. Phys. Lipids* 198, 21–27.
- Sierra, S., Ramos, M.C., Molina, P., Esteo, C., Vázquez, J.A., Burgos, J.S., 2011. Statins as neuroprotectants: a comparative *in vitro* study of lipophilicity, blood-brain-barrier penetration, lowering of brain cholesterol, and decrease of neuron cell death. *J. Alzheimers Dis.* 23, 307–318.
- Slater, E.E., MacDonald, J.S., 1988. Mechanism of action and biological profile of HMG CoA reductase inhibitors. A new therapeutic alternative. *Drugs* 36, 72–82.
- Stosel, T.P., 2008. The discovery of statins. *Cell* 134, 903–905.
- Stubbs, C.D., Ho, C., Slater, S.J., 1995. Fluorescence techniques for probing water penetration into lipid bilayers. *J. Fluoresc.* 5, 19–28.
- Thewalt, J.L., Bloom, M., 1992. Phosphatidylcholine: cholesterol phase diagrams. *Biophys. J.* 63, 1176–1181.
- Van Aelst, L., D'Souza-Schorey, C., 1997. Rho GTPases and signaling networks. *Genes Dev.* 11, 2295–2322.
- van Meer, G., Voelker, D.R., Feigenson, G.W., 2008. Membrane lipids: where they are and where they behave. *Nat. Rev. Mol. Cell Biol.* 9, 112–124.
- Wood, W.G., Eckert, G.P., Igbavboa, U., Müller, W.E., 2010. Statins and neuroprotection. A prescription to move the field forward. *Ann. N. Y. Acad. Sci.* 1199, 69–76.
- Wu, H., Lu, D., Jiang, H., Xiong, Y., Qu, C., Li, B., Mahmood, A., Zhou, D., Chopp, M., 2008. Increase in phosphorylation of Akt and its downstream signaling targets and suppression of apoptosis by simvastatin after traumatic brain injury. *J. Neurosurg.* 109, 691–698.
- Wu, H., Mahmood, A., Qu, C., Xiong, Y., Chopp, M., 2012. Simvastatin attenuates axonal injury after experimental traumatic brain injury and promotes neurite outgrowth of primary cortical neurons. *Brain Res.* 1486, 121–130.